



## ANALYZING THE EFFECT OF POSITION OF ANEURYSMAL SAC IN AN ATHEROSCLEROTIC CORONARY ARTERY USING A 2D MATHEMATICAL MODEL

S. SHANKAR NARAYAN<sup>1</sup>, ANURADHA BHATTACHARJEE<sup>2</sup>  
and SUNANDA SAHA<sup>3</sup>

<sup>1,2</sup>Dayananda Sagar University  
Bengaluru, India – 560068  
CMR Institute of Technology  
Bengaluru, India- 560037

<sup>3</sup>Bengaluru, India – 560037  
Vellore Institute of Technology  
Vellore, India – 632014 S.S.N  
E-mail: anuradha-math@dsu.edu.in  
sunanda.saha@vit.ac.in

### Abstract

The presence of an aneurysmal sac in a stenosed artery in the vicinity of the stenosis inflammation affects the blood flow characteristics in the artery. In the present paper, we intend to investigate the changes in the flow characteristics of blood in an arterial segment equivalent to the coronary arterial segment. We analyze the flow characteristic alterations by varying the position of the aneurysmal sac with respect to the stenosis in an arterial segment. The study revealed the spots on the arterial inner wall vulnerable to undergo endothelial dysfunction. The explanation about the various possible locations of sac-lump pairs is presented in the manuscript. This adds novelty to the present research article. The investigation of the sac-lump topography along the arterial wall can aid in understanding the proximity of a sac to undergo a blowout.

---

2020 Mathematics Subject Classification: 35A08, 76A05, 92C10.

Keywords: Aneurysm, Stenosis, Velocity profile, Wall Shear Stress, Endothelium.

<sup>1</sup>Corresponding author; E-mail: shankar.n@cmrit.ac.in

Received September 7, 2021; Accepted October 26, 2021

## 1. Introduction

Inherited conditions or the complications like high blood pressure and the habit of smoking among individuals leave a weakened arterial wall in the vascular system. Due to the weakened arterial wall, the pressure exerted by the blood on the wall results in the ballooning out of the arterial walls outwards. This condition is termed the “Aneurysm”. Most common aneurysms are seen in the cranial nerves. It is seen that out of 100 patients undergoing coronary angioplasty, 0.3% to 5% of them are identified with the coronary aneurysmal condition (Gundodu et al., [9]). Coronary aneurysms are normally without symptoms. The origin of these aneurysmal occurrences is investigated to be atherosclerosis in the majority of the cases (Golledge and Norman, [8]). Extreme pressure caused the rupture of the aneurysmal sac. The rupture of these sacs can lead to the discharge of blood into the neighboring tissues causing thrombosis and finally may even cause death. Arteries with multiple aneurysms or with the daughter sacs have more probability to undergo the eruption (Lev and Gonzalez, [12]).

Build up of Low-Density Lipoproteins (LDL) on the inner arterial wall, leading to the blockage for the flow of blood across the arterial segment inaugurates the condition called “Atherosclerosis” (Raggi et al., [13]). The occurrence of the sediments of the LDL on the arterial wall disturbs the geometry of the arterial segment leading to drastic changes in the flow characteristics of blood. These changes in blood rheology lead to various pathological conditions. Due to the deposition of LDL, the seepage of nutrients and oxygen into the cells of the arterial wall is disrupted leading to the weakening of the wall. The sudden pressure gradient caused due to the interrupting stenosis can result in ballooning. At some time the pressure in the middle of the blood vessel, the tension of the wall, and the strength of the wall itself have a connecting balance. When it reaches this point, the wall begins to grow in size in the plaque area. The vessel’s diameter rises, which leads to further dilatation, with the wall tension increased. An aneurysm is a result (Johnsen et al., [10]).

Assuming that atherosclerosis and aneurysms are interrelated to each other, we analyze the effects of changing the distance between these two pathologic conditions in an arterial segment generated computationally using

the Finite Element Method (FEM) solver. In the present paper, the investigation has been made on the flow characteristics of the blood in an arterial segment similar to the coronary arterial segment. The variables under the inquiry are the velocity and pressure profiles, Wall Shear Stress (WSS). As the blood has the property of changing the viscosity regulated by the geometry of the arteries, we treat the nature of blood to be non-Newtonian (Vinoth R, Kumar D, [17]).

In section 2 of the present manuscript, the mathematical model considered for the present study has been framed. The methodology used to solve the model has been explained. In section 3, the simulation results obtained by solving the model using a FEM solver are presented. In the following section, the manuscript has been concluded by suggesting the possible future developments of the present study.

The main conclusions of the present research are:

- The geometrical orientation of the aneurysmal and the stenosis lumps have a greater impact on the bursting of the aneurysmal sac due to the modifications seen in the flow characteristics of blood.
- The position of the stenosis past the aneurysmal sac affects the flow whereas the interchange of the positions of the sac and lump horizontally along the channel does not accost any reconditioning of the flow.
- The wall inner to the aneurysmal sac experiences a low wall shear stress. Thus, the innermost layer of the arterial wall in an aneurysmal sac has a more probability to develop a new sac, preferably named a “Daughter sac”.

## 2. Mathematical Model and the Methodology

The flow of blood in the coronary arterial segment considered for the present study is governed by the standard Navier Stokes equation coupled with the Continuity equation. The following assumptions are made while framing the model:

- The flow is incompressible.
- The flow is laminar.

• As the cardiac activity is time-dependent, the periodic study has been taken into consideration for the present investigation (Wu et al., [18]).

• Blood is a non-Newtonian fluid (Udupa et al., [16]).

• The only driving force for the flow of blood from the inlet to the outlet boundary is the pressure gradient.

• The walls of the arterial segment are inelastic.

The mathematical model examined is:

$$[\partial u / \partial t + \rho(u \cdot \nabla)u] + \nabla p - \text{div}(\tau) = f$$

$$\nabla \cdot u = 0$$

where  $u$  is the velocity of blood,  $\rho$  is the density of blood,  $p$  represents the pressure,  $\tau$  denotes the stress and  $f$  denotes the source term.

The non-Newtonian model employed for the present study is the Carreau model for non-Newtonian viscosity, as it covers both the Newtonian and non-Newtonian nature depending on the shear rates (Akbar and Nadeem, 2014). The stress tensor is given by  $\tau = \mu(\dot{\gamma})\dot{\gamma}$  where  $\mu$  denotes the blood viscosity as a function of shear rate.

$$\mu = \mu_{\infty} + (\mu_0 - \mu_{\infty})[1 + (\lambda\dot{\gamma})^2]^{(n-1)/2}$$

where  $\mu_0$  is the zero shear viscosity,  $\mu_{\infty}$  is the infinite shear viscosity,  $n$  and  $\lambda$  are model parameters.

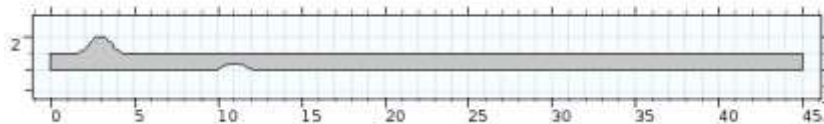


**Figure 1.** Sample geometry under the present study.

The geometry used for the investigation is shown in figure 1. The properties of the geometry, the values of the physical parameters, and the boundary conditions are defined in table 1. Figure 2 represents the graphical plot of the function  $f(t)$ .

**Table 1.** Properties of the geometry, the values of the physical parameters, and the boundary conditions.

Particulars	Values	References
Geometry Details		
Length of the arterial segment	45mm	(S and Saha, [14])
Diameter of the arterial segment	1 mm	
Percentage of stenosis	45 %	
Diameter of the aneurysm	1 mm	
Parameter values of non-Newtonian Model		
Zero shear viscosity, $\mu_0$	0.0456 Pa s	(Boujena et al., 2014)
Infinite shear viscosity, $\mu_\infty$	0.0032 Pa s	
Model parameter, $n$	0.344	
Model parameter, $\lambda$	10.03 s	
Blood properties		
The density of blood, $\mu$	1060 Kg/m <sup>3</sup>	(Boujena et al., 2014)
Boundary Conditions		
Initial Velocity	0.3 m/s	

Relative velocity and pressure function, $f(t)$	$\begin{cases} (1 - \alpha) \sin \pi t, & 0s \leq t \leq 0.5s \\ 1 - \alpha \cos(2\pi(t - 0.5)), & 0.5s \leq t \leq 1.25s \end{cases}$	(Choudhari and Panse, 2016)
Relative velocity amplitude ( $\alpha$ )	1/5	
Inlet velocity	0.3 [m/s] $*f(t)$	
Outlet pressure	125 [mmHg] $*f(t)$	

Different cases under study are enlisted below:

### I. Aneurysm on the upper wall and Stenosis on the lower wall

Fixing the aneurysmal sac and varying the position of atherosclerosis: Aneurysm centered at 3 mm, stenosis centered at 3 mm, 6 mm, 9 mm, and 12 mm. (Cases 1,2,3, and 4 respectively).

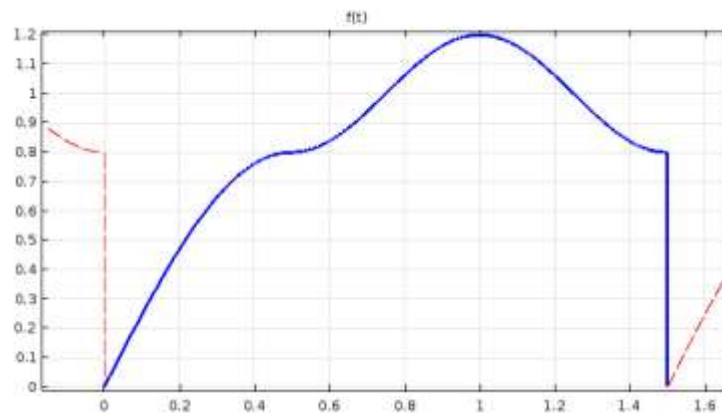


Figure 2. Graph of  $f(t)$ .

### II. Aneurysm on the upper wall and Stenosis on the upper wall

Aneurysm centered at 3 mm, stenosis centered at 6 mm, 9 mm, and 12 mm. (Cases 5, 6, and 7 respectively).

### III. Interchanging the position of aneurysm and stenosis

An aneurysm is located before the stenosis (case 8- identical to case 3) and Stenosis is located before the aneurysm (case 9).

Adopting the above-mentioned values for the model, model validation has been done to check the correctness of the model. The validation results are verified using the previously published articles (Cilla et al., [6], S and Saha, [14], Silva et al., [15]).

As an initial step in the simulation, the mesh construction has been made over the domain under the consideration. A Mesh independence test has been conducted to select the suitable mesh configuration. For the present study, a Fine meshing configuration is applied as a result of the mesh independence test, as seen in figure 3. The details of the mesh elements are mentioned in table 2. The meshing quality of the fine mesh constructed is presented in figure 4.

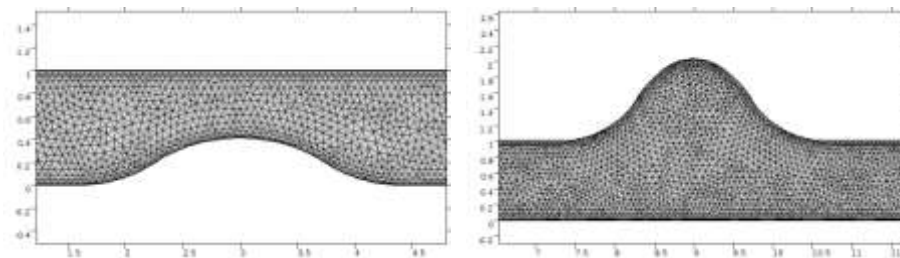


Figure 3. Fine meshing near stenosis and aneurysmal sac respectively.

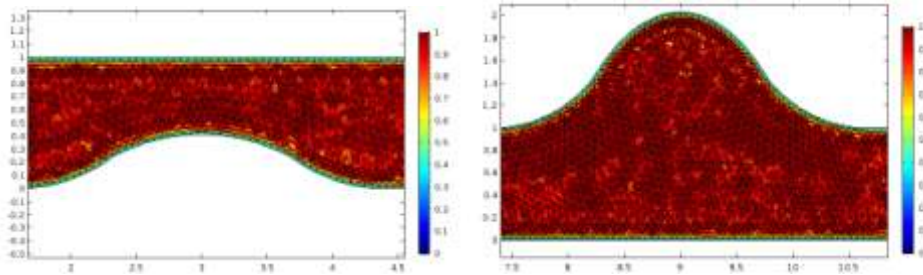


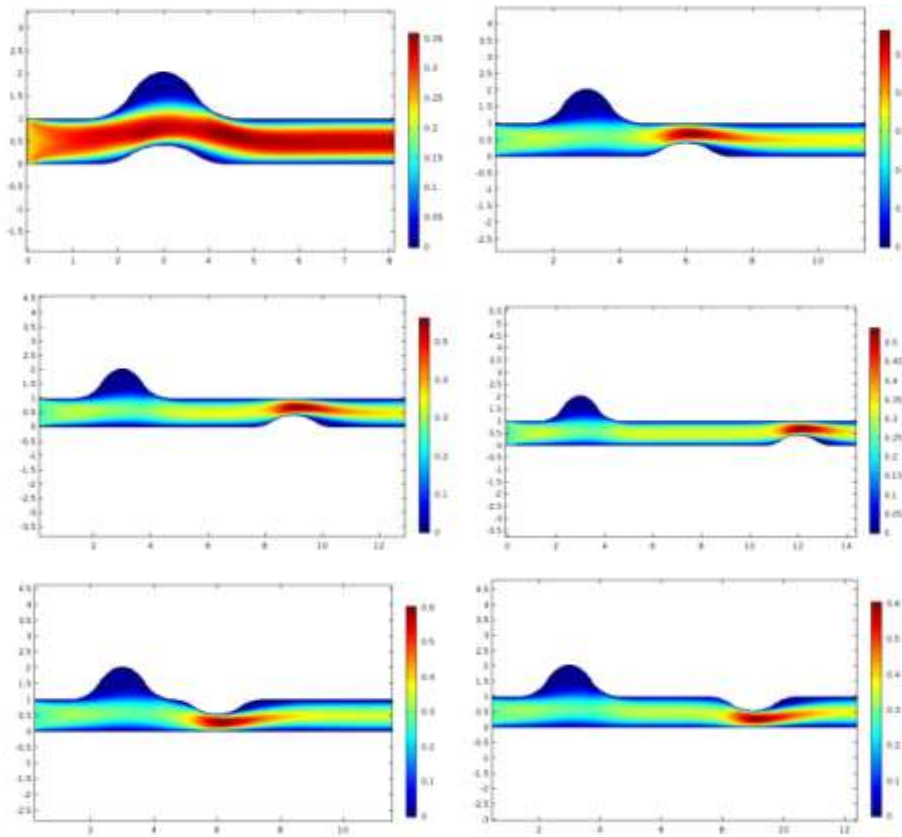
Figure 4. Fine meshing quality near stenosis and aneurysmal sac respectively.

Table 2. Mesh Element Details.

Case Number	Triangular elements	Quadrilateral elements	Edge elements	Vertex elements	Minimum element quality	Average element quality	Element area ratio
-------------	---------------------	------------------------	---------------	-----------------	-------------------------	-------------------------	--------------------

(i)	25355	3194	1631	14	0.3232	0.8581	0.06885
(ii)	25488	3194	1632	14	0.3231	0.8626	0.07476
(iii)	25479	3194	1631	12	0.3233	0.8627	0.07658
(iv)	29165	3194	1631	12	0.07432	0.807	0.03093
(v)	26233	3354	1715	13	4.271E-4	0.8528	5.271E-7
(vi)	25405	3198	1633	13	0.327	0.8609	0.08012
(vii)	25416	3196	1632	13	0.3286	0.8629	0.07958
(viii)	25479	3194	1631	12	0.3233	0.8627	0.07658
(ix)	25590	3192	1630	12	0.3275	0.8616	0.05836

### 3. Results



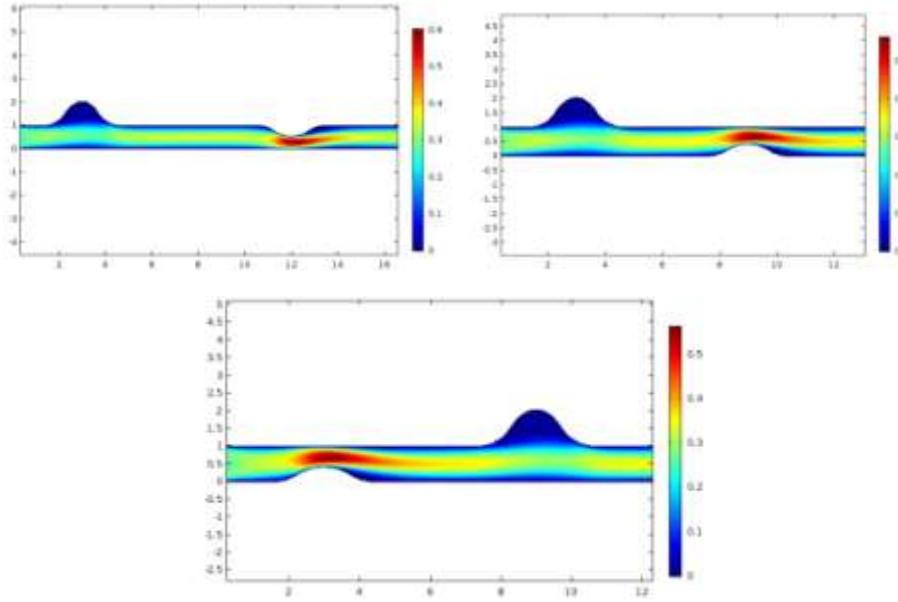
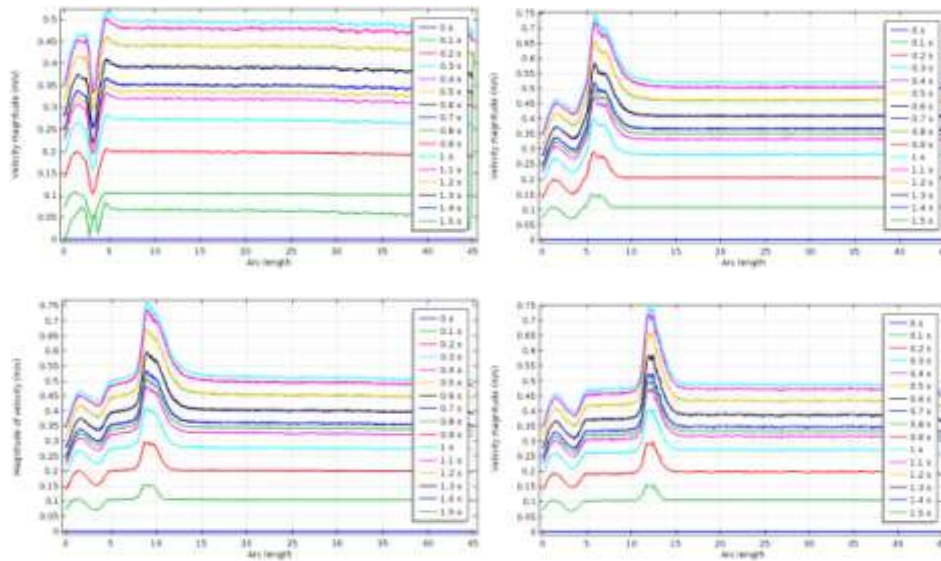


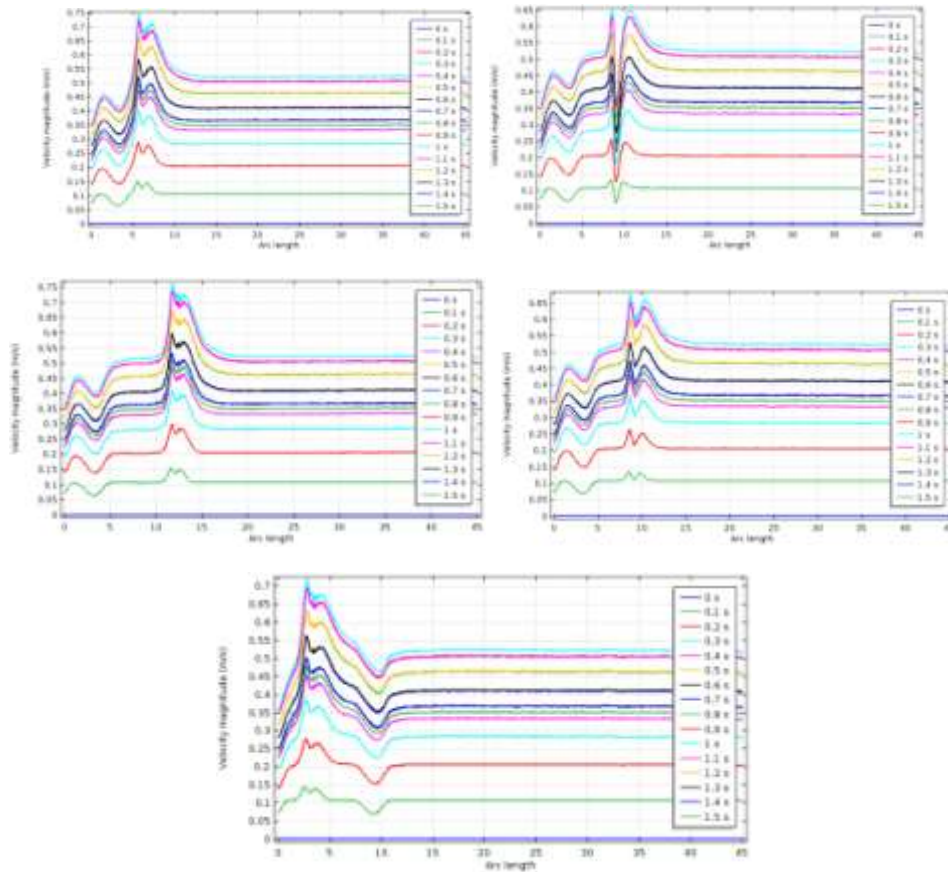
**Figure 5.** Two-dimensional Velocity profile for cases *i* to ix respectively.

The plots in figure 5 represent the two-dimensional simulation results for velocity in the flow channel for different cases under the current study. At the narrowed region of the arterial segment, due to the sedimentation of LDL, peak velocity is noticed in all the cases. The decrease in the diameter at these cramped regions leads to the rise in the kinetic energy of the blood (Bajpai, [2]). At the regions of aneurysmal sacs, the blood confronts the broader area due to the presence of extraneous area provided by the sacs. Due to the hasty change in the flow geometry, blood velocity decreases following Bernoulli's principle for hydraulics. But for case 1, in which the stenosis lump is right below the aneurysmal sac, the blood suffers a deviation in its path into the aneurysmal sac due to the protrusion of the stenosis nodule into the sac. This results in a high-pressure region inside the aneurysmal sac, leading to a drop in velocity (Maximum velocity reached is seen to be 0.35 m/s, which is appreciably low when compared to the other cases) (Konishi et al., [11]). Hence, the probability of the blast of the sac in case 1 is much higher when compared to the other cases under research. The cases from 2 to 9 can lead to case 1 due to the low-velocity profile near the aneurysmal sac location. Further, it can be observed that in the case when the stenosis is located in the upper wall next to the aneurysmal sac, there is a considerable rise in the

magnitude of velocity below the stenosis along the axis of the flow channel. This is because in these cases blood is maintained flow over the same plane. There is no change in the plane of motion for blood in cases 5, 6 and 7. Ultimately, we can also notice that there is no difference in the flow pattern among the eventual cases 8 and 9. Thus, it can be concluded that the position of the stenosis past the aneurysmal sac affects the flow whereas the interchange of the positions of the sac and lump horizontally along the channel does not accost any reconditioning of the flow.

Plots in figure 6 mirror the velocity curves for the cases under deliberation. Due to the overlap of the region above the stenosis nodule and the region below the aneurysmal sac, a deep dip is seen in the velocity of case 1. Immediately after passing the common region, the velocity recovery is seen from the graph to maintain the necessary pressure. The graphs of cases 2, 3, 4, 8, and 9 are seen to be similar to each other with a velocity drop at the region below the sac and a rise in the value above the stenosis lump. A noticeable difference is seen in cases- 5, 6 and 7, due to the presence of the stenosis lump along the same wall as that of the sac.

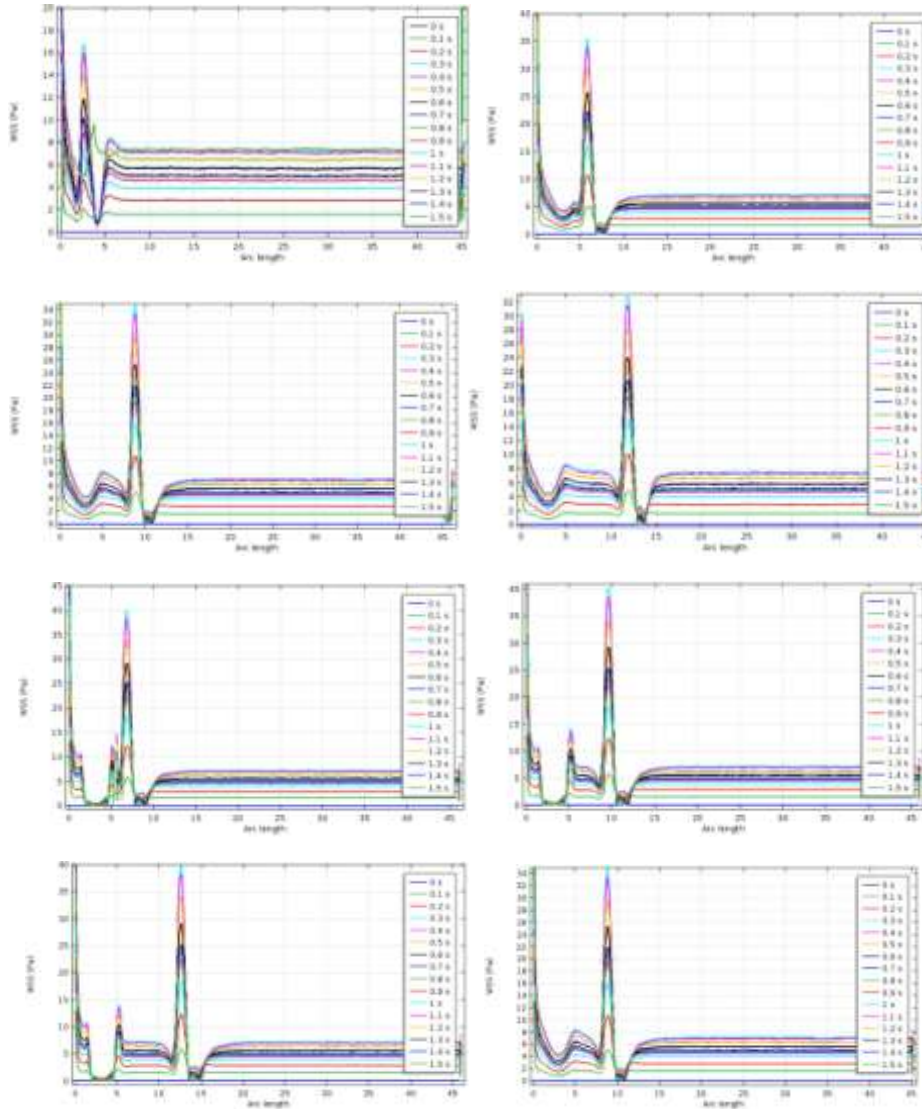


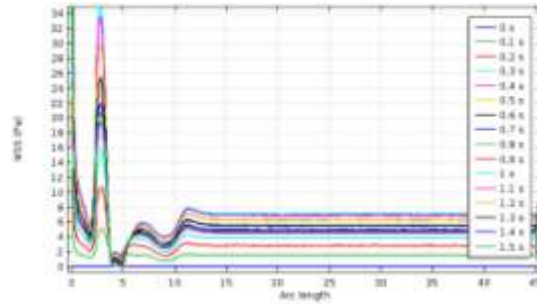


**Figure 6.** Axial velocity curves for cases *i* to *ix* respectively.

Low or fluctuating shear stress appears to be the best environment for LDL to accumulate and atherosclerotic lesions to form. The frictional force produced by the circulating blood column on the intimal surface of the arteries is known as wall shear stress. The plots of figure 7 are the WSS curves for the various cases under study. The plots of WSS acknowledge the possible sites for the future development of stenosis or the aneurysms because the low or the oscillatory WSS regions undergo the dysfunction of the endothelial layer of the intima leading to the wall weakening. This is proved clinically by the previously published articles (Boussel et al., [4], Dhawan et al., [7]). In case 1, the immediate neighboring region next to the stenosis lump experiencing the recirculation is seen to possess a low WSS value range, resulting in a suitable place for the growth of new plaque. A similar

conclusion can be made in cases 2,3,4,8 and 9. But in other cases, the wall inner to the aneurysmal sac experiences a low wall shear stress. Thus, the innermost layer of the arterial wall in an aneurysmal sac has a more probability to develop a new sac, preferably named a “Daughter sac”.

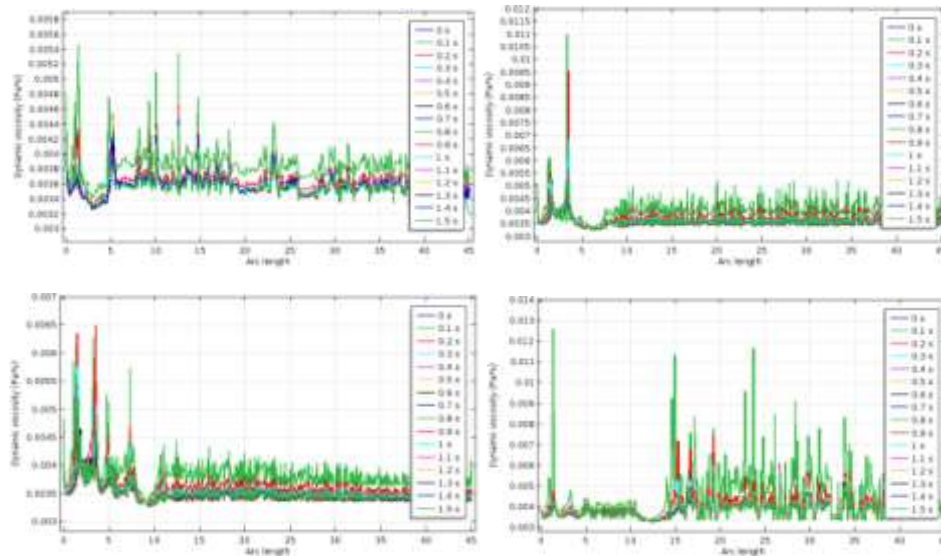




**Figure 7.** WSS profiles on the walls with stenosis for cases  $i$  to  $ix$  respectively.

The plots in figure 8 depict the viscosity curves obtained along the axis of the flow channel. The graphs support the selection of the non-Newtonian model, the Carreau model, to mathematically model the blood.

The regions facing the hardship of reduction in the diameter, due to the shear rate exerted, violence the blood to embrace the non-Newtonian viscosity. The regions with the normal healthy arterial diameter treat the blood as a Newtonian fluid (Udupa et al., [16]). The plots of figure 8 afford the Newtonian property to blood in the healthy dimensions whereas fluctuating viscous values, non-Newtonian property, near the lumps.



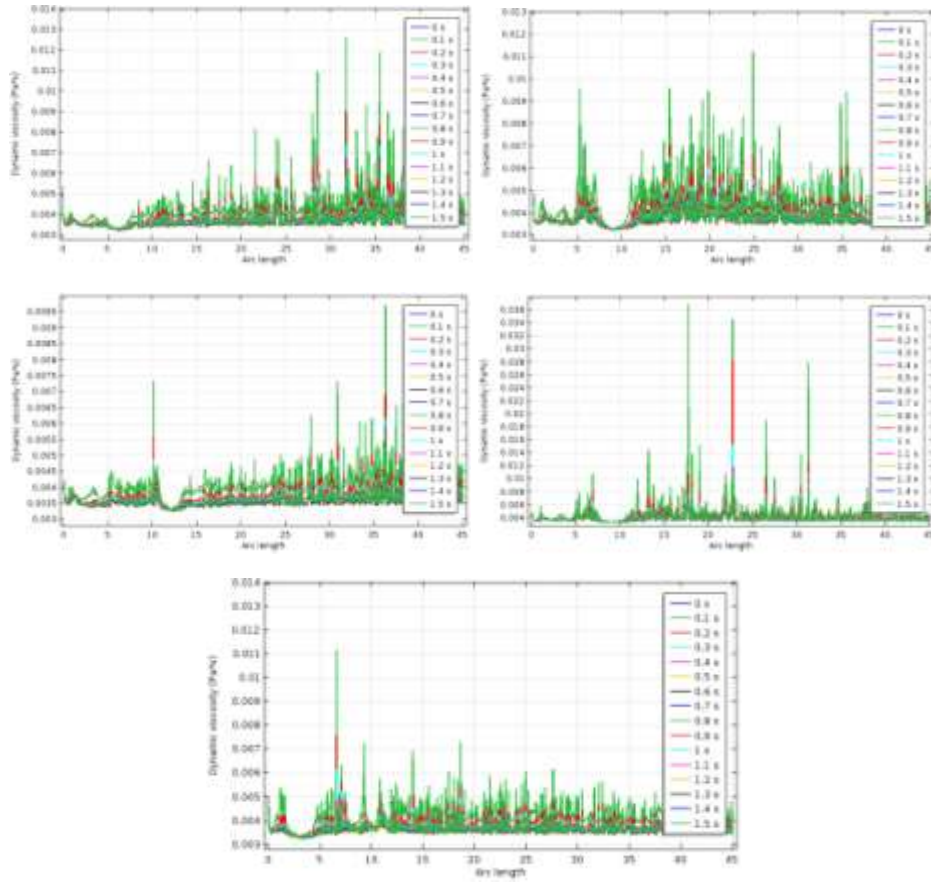
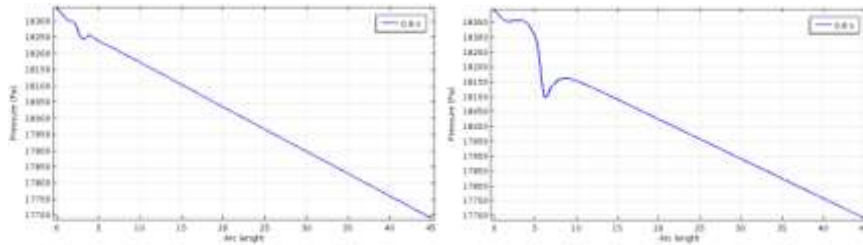
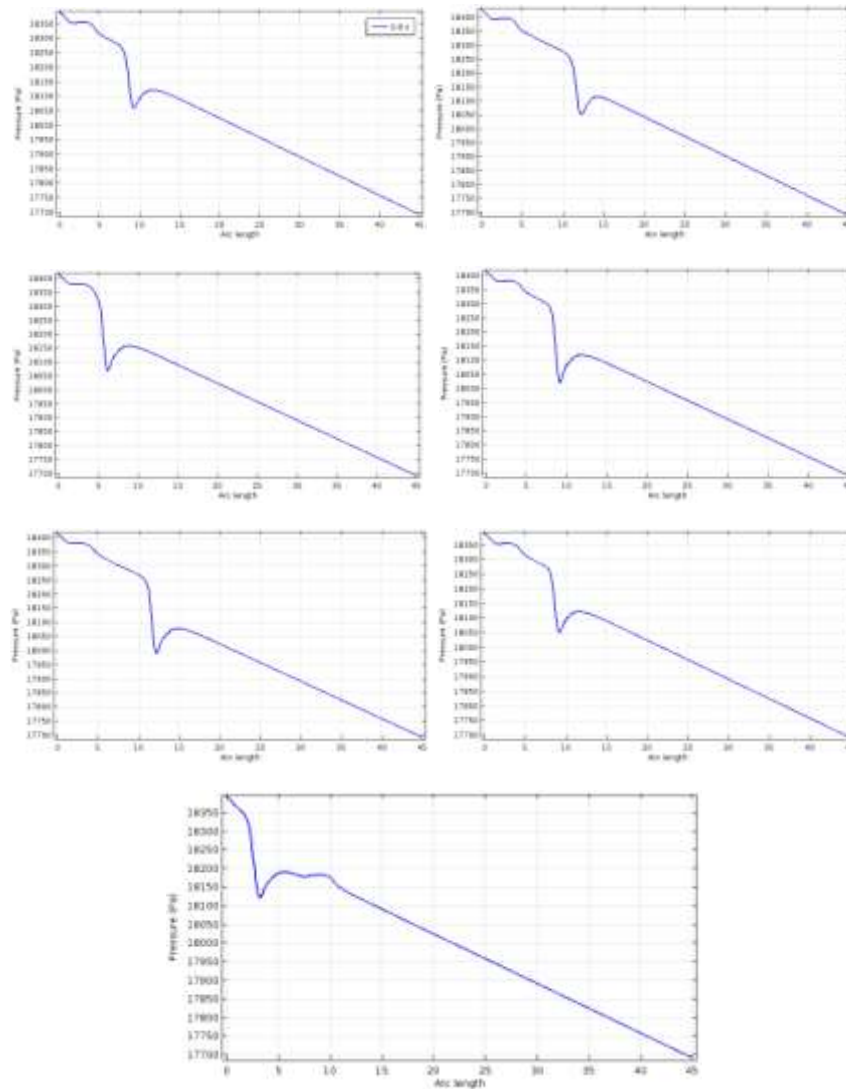


Figure 8. Axial viscosity curves for cases  $i$  to  $ix$  respectively.





**Figure 9.** Axial pressure for cases  $i$  to  $ix$  respectively at 0.8 s.

Subsequently, the plots in figure 9 are the pressure curves measured along the axis of the flow channel. To balance the total energy, the pressure varies inversely as the velocity along the flow channel. These curves are obtained at  $t = 0.8s$ . The graphs show an extensive reduction in the pressure near the stenosis regions and the reverse is noticed in the vicinity of the sacs. In case 1, there is the least drop in pressure so is the rise near the sac,

leading to the fact that the pressure exerted by blood over the arterial wall inner to the sac makes the aneurysmal sac vulnerable for a blowout. Cases 2,3,4 follow the pressure drop pattern in the following order: Case 4 > Case 3 > Case 2. The greater pressure gradient invites easy wall weakening in downstream flow. The maximum pressure gradient is encountered in cases 5,6, and 7. Also, the drop is seen fewer in case 8 when compared to 9.

Summing the effects of the various flow attributes of blood, the following conclusion can be made:

- The threat of the blowout is maximum in case 1.
- The position of stenosis attached to the lower and the upper wall greatly affects the blood flow quirks.
- The interchange of the position of sac and lump has the least changes in the flow attributes.

#### 4. Conclusions

The present research article exposed the various changes in the flow characteristics induced due to the shifts in the position of the stenosis plaque with respect to the position of aneurysmal sacs and vice versa. The study investigated the flow of blood in nine different explorations concerning the permutations of the sac-lump locations. The study revealed the cases under threat for the detonation of the sac or the growth of new plaques. The study, being theoretical, considered possible locations for sac and lump. The possibility of these locations must be verified clinically using various angiographic techniques of the arterial systems. The results obtained can be analyzed in accordance with the clinical data for further examination.

#### References

- [1] N. S. Akbar and S. Nadeem, Carreau fluid model for blood flow through a tapered artery with a stenosis. *Ain Shams Engineering Journal* 5(4) (2014), 1307-1316. <https://doi.org/10.1016/j.asej.2014.05.010>
- [2] P. Bajpai, In Biermann's Handbook of Pulp and Paper, Hydraulics (2018), 455-482. <https://doi.org/10.1016/B978-0-12-814238-7.00023-4>
- [3] S. Boujena, O. Kafi and N. El. Khatib, A 2D Mathematical Model of Blood Flow and its Interactions in an Atherosclerotic Artery, *Math. Model Nat. Phenom* 9(6) (2014), 46-68. <https://doi.org/10.1051/mmnp/20149605>

- [4] L. Boussel, V. Rayz, C. McCulloch, A. Martin, G. Acevedo-Bolton, M. Lawton, R. Higashida, W. S. Smith, W. L. Young and D. Saloner, Aneurysm growth occurs at region of low wall shear stress: Patient-specific correlation of hemodynamics and growth in a longitudinal study, *Stroke* 39(11) (2008), 2997-3002. <https://doi.org/10.1161/STROKEAHA.108.521617>
- [5] P. Choudhari and M. S. Panse, Finite Element Modeling and Simulation of Arteries in the Human Arm to Study the Aortic Pulse Wave Propagation, *Procedia Computer Science* 93 (2016), 721-727. <https://doi.org/10.1016/j.procs.2016.07.277>
- [6] M. Cilla, E. Peña and M. A. Martínez, Mathematical modelling of atheroma plaque formation and development in coronary arteries, *Journal of the Royal Society Interface*, 11(90) (2014). <https://doi.org/10.1098/rsif.2013.0866>
- [7] S. S. Dhawan, R. P. A. Nanjundappa, J. R. Branch, W. R. Taylor, A. A. Quyyumi, H. Jo, M. C. McDaniel, J. Suo, D. Giddens and H. Samady, Shear stress and plaque development, In *Expert Review of Cardiovascular Therapy* 8 (2010), 545-556. <https://doi.org/10.1586/erc.10.28>
- [8] J. Golledge and P. E. Norman, Atherosclerosis and abdominal aortic aneurysm: Cause, response, or common risk factors? In *Arteriosclerosis, Thrombosis, and Vascular Biology*, 30 (2010) 1075-1077. <https://doi.org/10.1161/ATVBAHA.110.206573>
- [9] F. Gundodu, S. Arslan, E. Buyukkaya and H. Senocak, Treatment of a coronary artery aneurysm by use of a covered stent graft - A case report. *International Journal of Angiology* 16(1) (2007), 31-32. <https://doi.org/10.1055/s-0031-1278242>
- [10] S. H. Johnsen, S. H. Forsdahl, K. Singh and B. K. Jacobsen, Atherosclerosis in abdominal aortic aneurysms: A causal event or a process running in parallel? the tromsø study, *Arteriosclerosis, Thrombosis, and Vascular Biology* 30(6) (2010), 1263-1268. <https://doi.org/10.1161/ATVBAHA.110.203588>
- [11] Y. Konishi, K. Fukasaku, T. Kobori, Y. Takakura, N. Arai, H. Yazaki and Y. Shiokawa, Flow in a tube with an aneurysmal sac: Effect of aneurysm and stent. *Interventional Neuroradiology*, 12(SUPPL. 1) (2006), 53-56. <https://doi.org/10.1177/15910199060120s106>
- [12] M. H. Lev and R. G. Gonzalez, CT Angiography and CT Perfusion Imaging, In *Brain Mapping: The Methods* (2002), 427-484. <https://doi.org/10.1016/b978-012693019-1/50019-8>
- [13] P. Raggi, J. Genest, J. T. Giles, K. J. Rayner, G. Dwivedi, R. S. Beanlands and M. Gupta, Role of inflammation in the pathogenesis of atherosclerosis and therapeutic interventions, In *Atherosclerosis* 276 (2018), 98-108. <https://doi.org/10.1016/j.atherosclerosis.2018.07.014>
- [14] S. S. N. and S. Saha, Time-dependent study of blood flow in an aneurysmic stenosed coronary artery with inelastic walls, *Materials Today: Proceedings* (2021). <https://doi.org/10.1016/j.matpr.2021.05.608>
- [15] T. Silva, W. Jäger, M. Neuss-Radu and A. Sequeira, Modeling of the early stage of atherosclerosis with emphasis on the regulation of the endothelial permeability, *Journal of Theoretical Biology*, 496 (2020). <https://doi.org/10.1016/j.jtbi.2020.110229>

- [16] M. Udupa, S. Shankar Narayan and S. Saha, A Study of the Blood Flow Using Newtonian and Non-Newtonian Approach in a Stenosed Artery. *Advances in Intelligent Systems and Computing* 1169 (2021), 257-269. [https://doi.org/10.1007/978-981-15-5414-8\\_21](https://doi.org/10.1007/978-981-15-5414-8_21)
- [17] R. Vinoth, D. R. A. Kumar and V. S. C, Non-Newtonian and Newtonian blood flow in human aorta: A transient analysis, *Biomedical Research* 28(7) (2017).
- [18] J. Wu, G. Liu, W. Huang, D. N. Ghista and K. K. L. Wong, Transient blood flow in elastic coronary arteries with varying degrees of stenosis and dilatations: CFD modelling and parametric study, *Computer Methods in Biomechanics and Biomedical Engineering* 18(16) (2015), 1835-1845. <https://doi.org/10.1080/10255842.2014.976812>